Electronic Supplementary Material (ESI) for Nanoscale.

Supplementary Information

Colloidal Synthesis of Cu-ZnO and Cu@CuNi-ZnO Hybrid Nanocrystals with Controlled Morphologies and Multifunctional Properties

Deqian Zeng, Pingyun Gong, Yuanzhi Chen,* Qinfu Zhang, Qingshui Xie and Dong-Liang Peng*

Department of Materials Science and Engineering, Collaborative Innovation Center of Chemistry for Energy Materials, College of Materials, Xiamen University, Xiamen, 361005, People's Republic of China.

Synthesis of ZnO nanocrystals.

In a typical synthesis, 0.2 mmol of acetylacetone (2,4-pentadione) and 1.5 mmol of TOPO were added into a mixed solution containing 3 mL of OAm and 4 mL of BA, and heated at 70 °C for 10 min. After that, the mixed solution was heated up to 195 °C and kept at this temperature for 15 min, and then cooled down to 160 °C. In the next step, 0.55 mmol of $Zn(OAc)_2 \cdot 2H_2O$ and 2 mL of OAm were added into the above solution. Then the reaction mixture was heated up to 195 °C and kept at this temperature for 30 min before cooling down to room temperature naturally. After that, the precipitate was washed by mixed hexane, ethanol and acetone several times, separated from solution by centrifugation, and then dried in vacuum.

Ligand exchange of ZnO and ZnO-based photocatalysts. Before the photocatalytic experiment, the hydrophobic surfactants/ligands were exchanged by hydrophilic ligands. The ligand-exchange procedure was achieved by using imidazole solution based on previous report.[1, 2] Typically, ZnO or ZnO-based hybrid nanocrystals (25 mg) were dissolved in 20 mL of $CHCl_3$ and mixed with 20 mL of imidazole solution (5 mg/mL). The solution was strongly stirred for 20 min at room temperature under inert atmosphere (argon gas), and were isolated by centrifugation and subsequent washed twice with ethanol, and then dried in vacuum.

Photocatalytic tests. In the photocatalytic experiments, 10 mg of the sample was suspended in 100 mL RhB aqueous solution (0.01 g/L), and then the aqueous suspension was agitated in the dark for 1 h to reach adsorption–desorption equilibrium of the dyes on the surfaces of

photocatalyst. Subsequently, the mixture was irradiated using a 175 W UV lamp (major wavelength 365 nm). To determine the degradation percentage of RhB as a function of time at different intervals, 3.0 mL aliquots of the suspension were collected and centrifuged for 10 min at a rate of 3000 rpm, and then the absorbance of the RhB solution was measured using a Shimadzu UV-2550 ultraviolet-visible spectrophotometer.

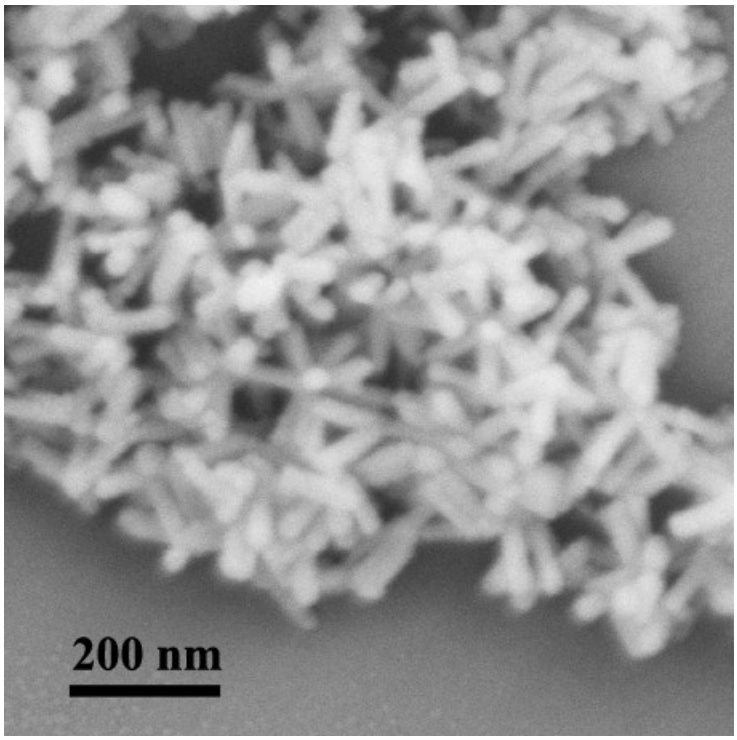

Fig. S1 SEM image of Cu-ZnO hybrid nanomultipods.

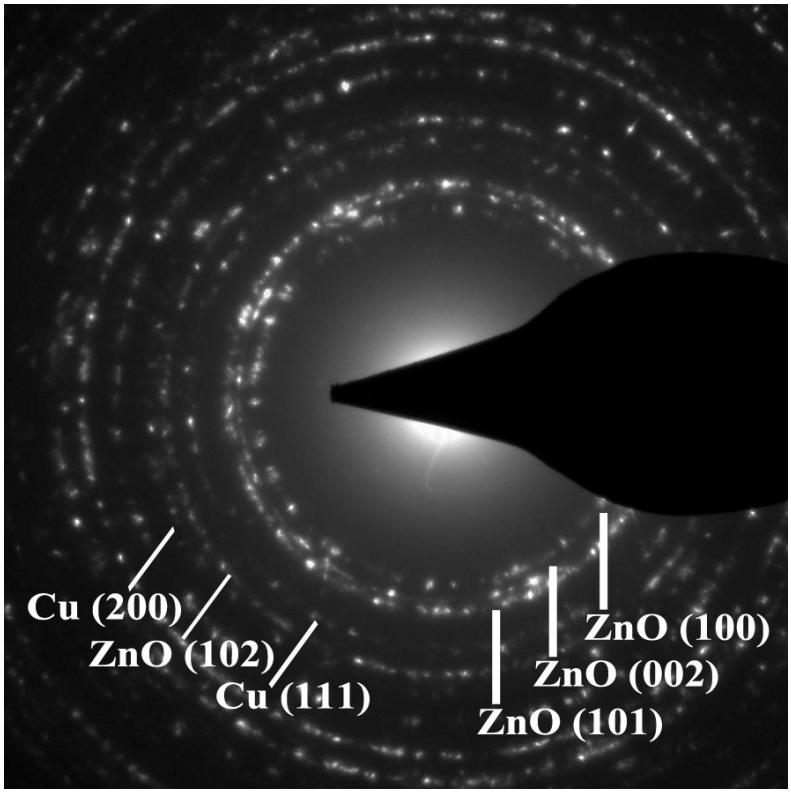

Fig. S2 SAED pattern of Cu-ZnO hybrid nanomultipods.

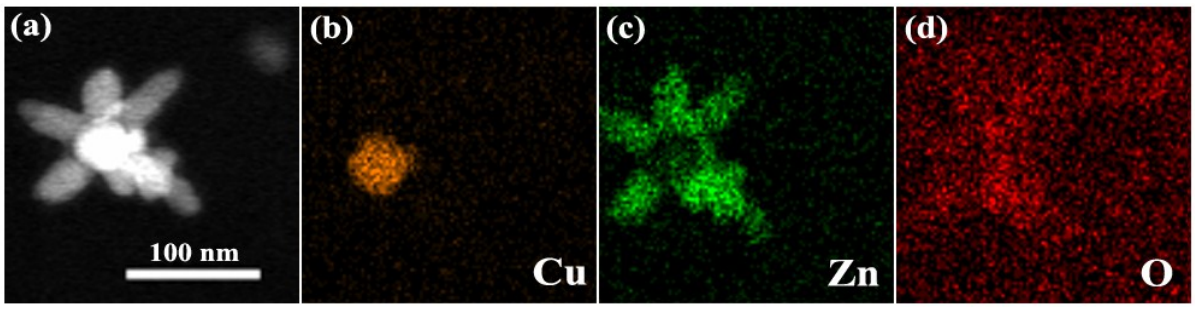

Fig. S3 HAADF image (a) along with elemental maps of Cu (b), Zn (c) and O (d) for Cu-ZnO hybrid nanomultipods.

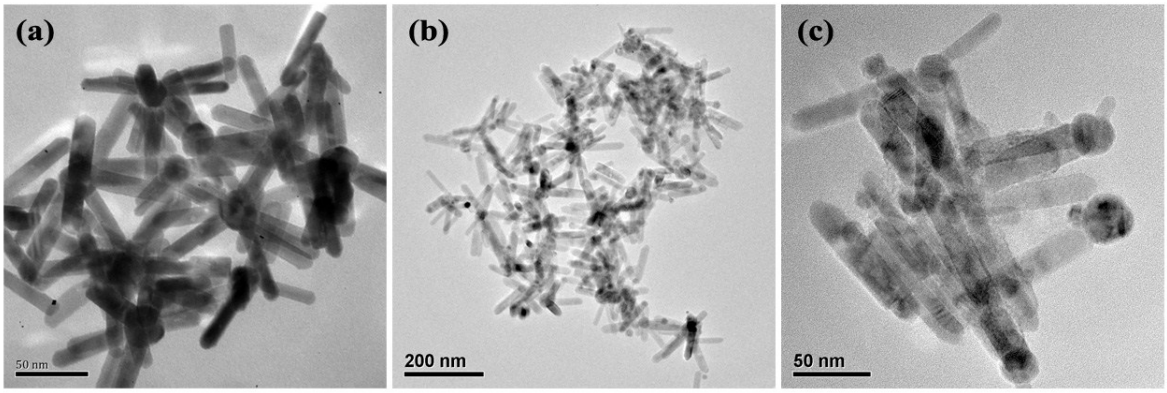

Fig. S4 TEM images of Cu-ZnO hybrid nanomultipods synthesized with 5 mL of OAm and 4 mL of BA (a), 7 mL of OAm and 4 mL of BA (b), and 10 mL of OAm and 4 mL of BA (c).

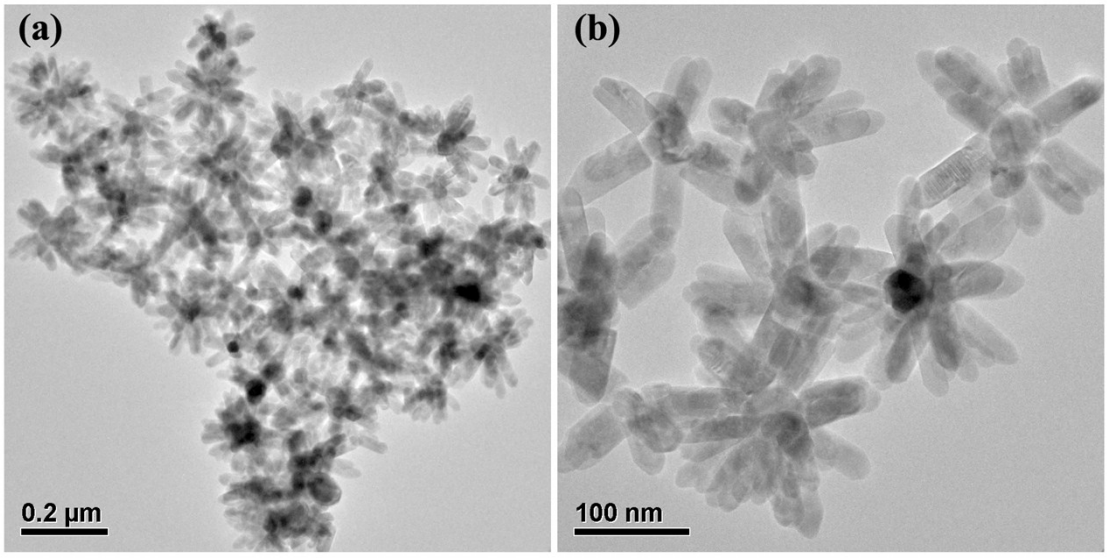

Fig. S5 TEM images of Cu-ZnO hybrid nanomultipods synthesized with 0.75 mmol of $Zn(OAc)_2 \cdot 2H_2O$.

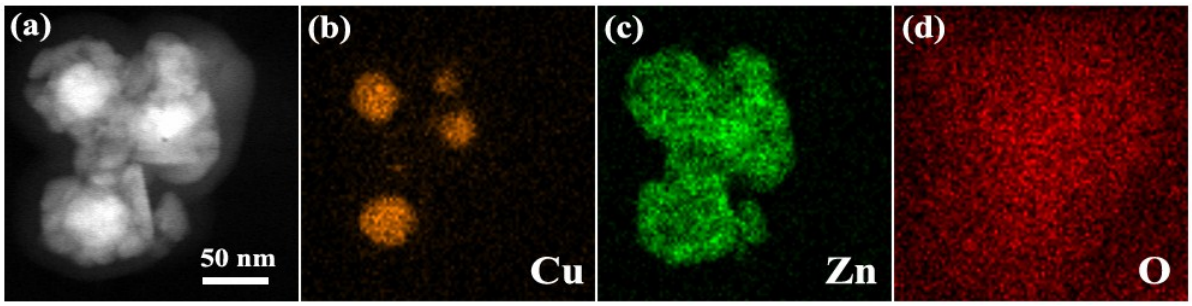

Fig. S6 HAADF image (a) along with elemental maps of Cu (b), Zn (c) and O (d) for Cu-ZnO core-shell nanoparticles.

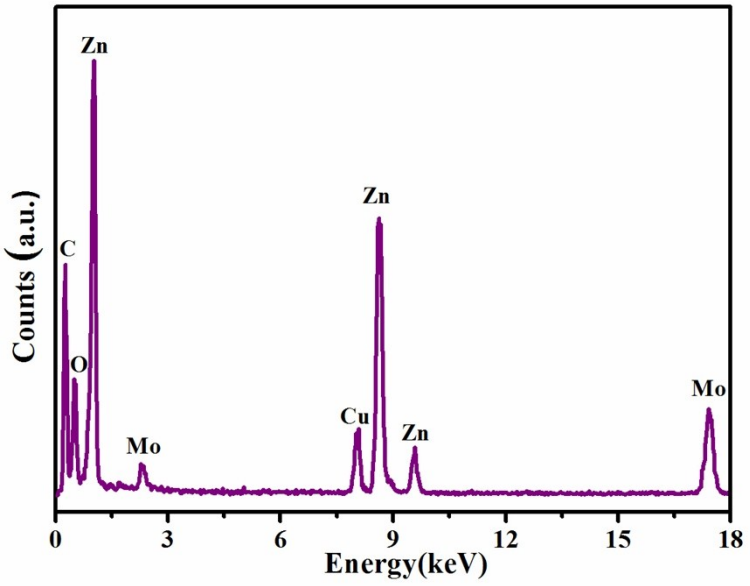

Fig. S7 EDS spectrum of an individual Cu-ZnO hybrid nanopyramid.

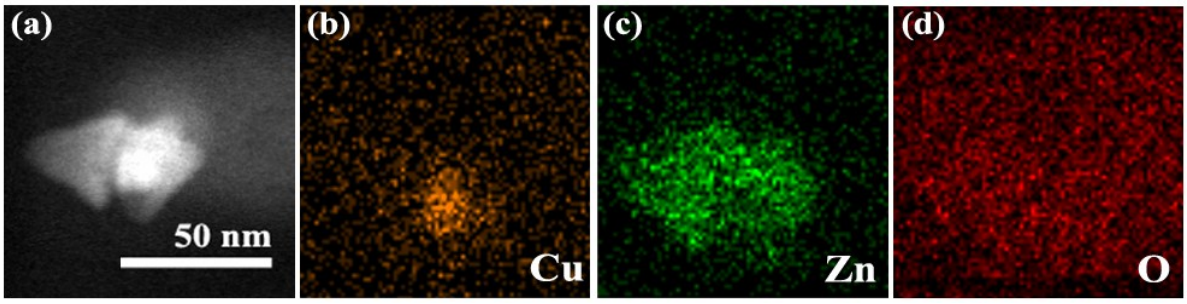

Fig. S8 HAADF image (a) along with elemental maps of Cu (b), Zn (c) and O (d) for Cu-ZnO hybrid nanopyramid.

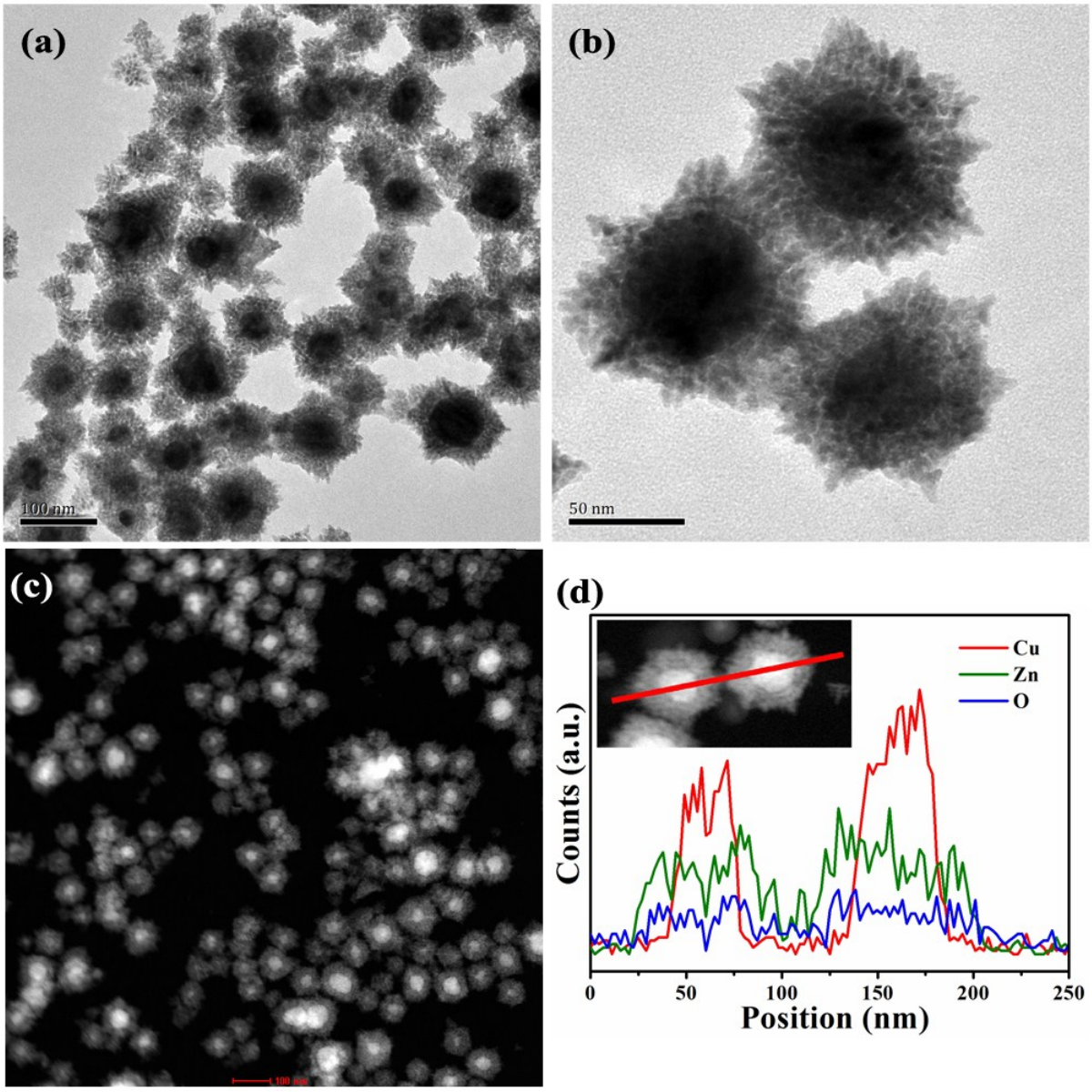

Fig. S9 Low-magnification TEM image (a), high-magnification TEM image (b), HAADF image (c) and STEM-EDS line-scan analysis (d) of Cu-ZnO core-shell nanocrystals using $Zn(St)_2$ instead of $Zn(OAc)_2 \cdot 2H_2O$ for the typical synthesis of Cu-ZnO nanomultipods.

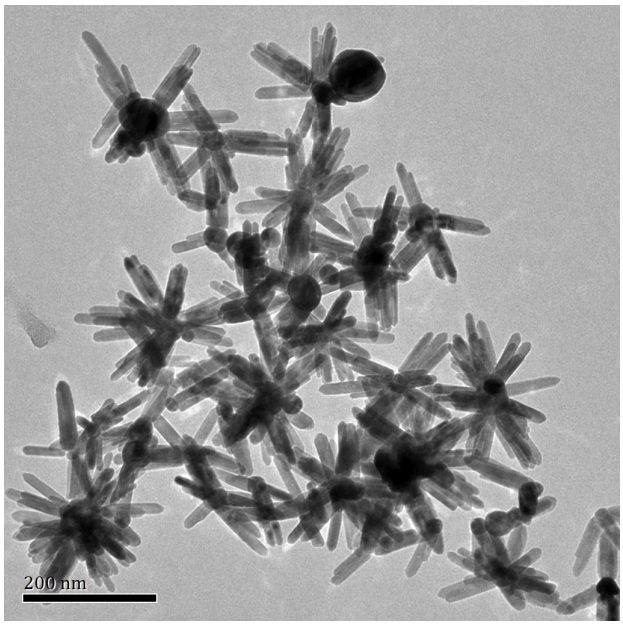

Fig. S10 TEM images of Cu-ZnO hybrid nanocrystals without adding TOPO for the typical synthesis of Cu-ZnO nanomultipods.

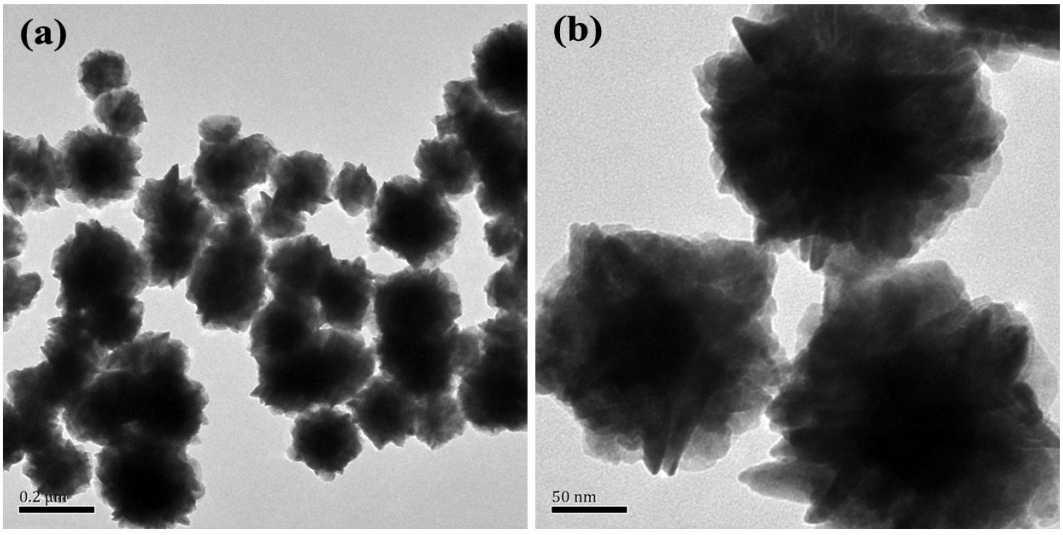

Fig. S11 Low-magnification TEM image (a) and high-magnification TEM image (b) of Cu-ZnO core-shell nanoparticles prepared using 5 mL of DBE instead of the mixture containing 2 mL of OAm and 3 mL DBE for the typical synthesis of Cu-ZnO core-shell nanoparticles.

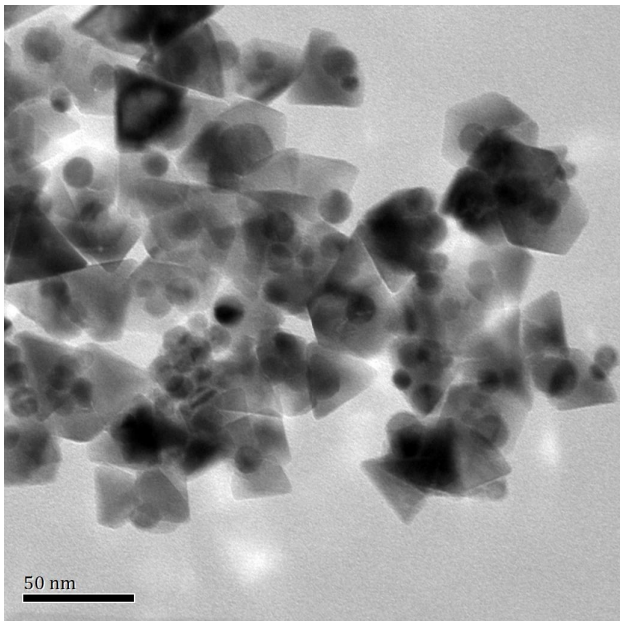

Fig. S12 TEM image of Cu-ZnO hybrid nanocrystals prepared using $Zn(St)_2$ instead of $Zn(OAc)_2 \cdot 2H_2O$ for the typical synthesis of Cu-ZnO core-shell nanoparticles.

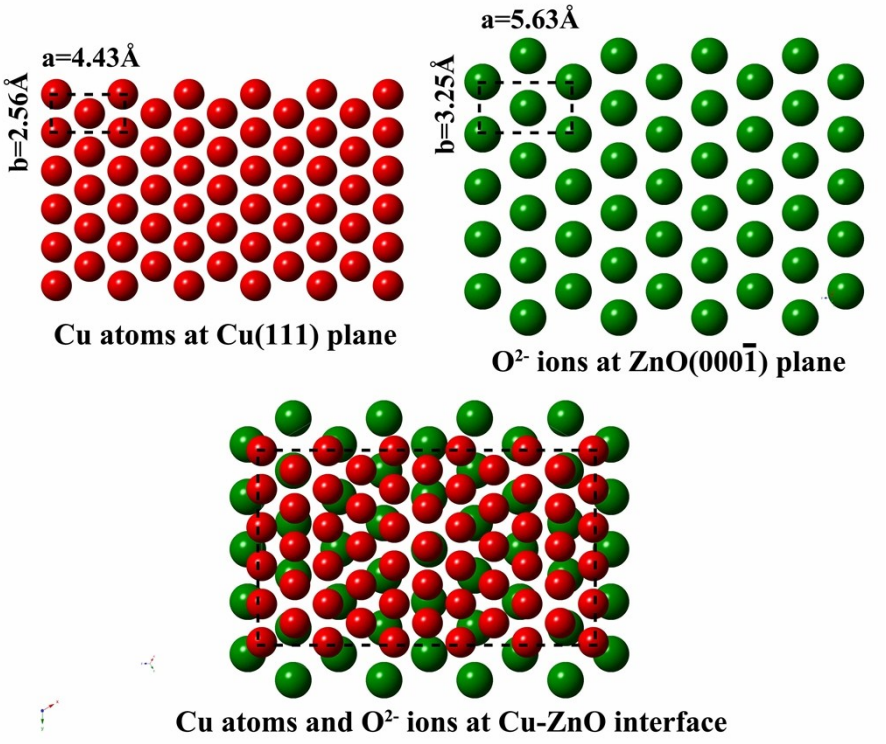

Fig. S13 Configurations of Cu atoms at Cu (111) plane, O^{2-} ions at ZnO $(000\bar{1})$ plane and Cu atoms and O^{2-} ions at Cu-ZnO interface.

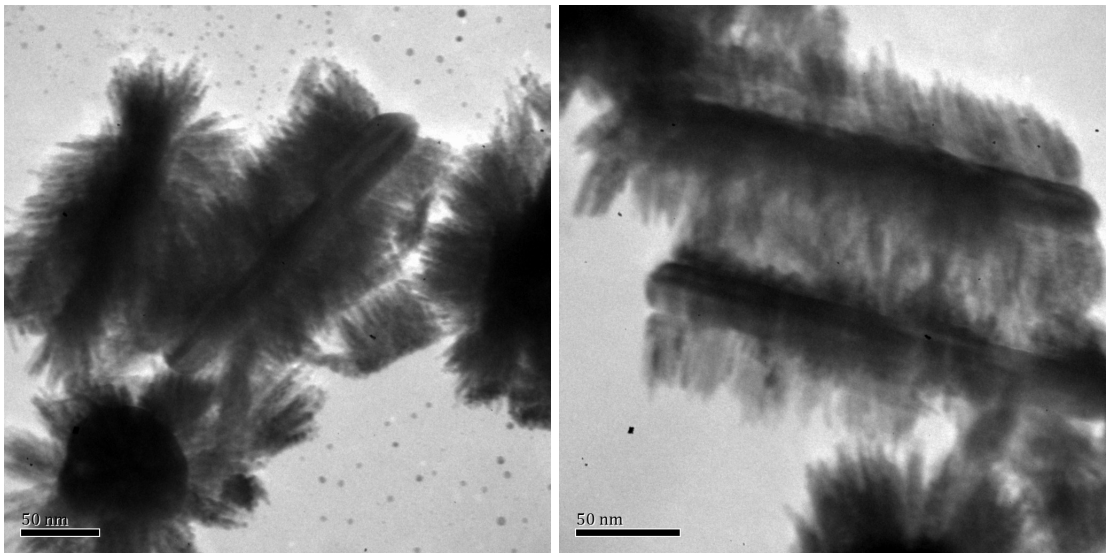

Fig. S14 TEM images of Cu-ZnO hybrid nanocrystals prepared using $CuCl_2$ instead of $Cu(acac)_2$ for the typical synthesis of Cu-ZnO nanomultipods.

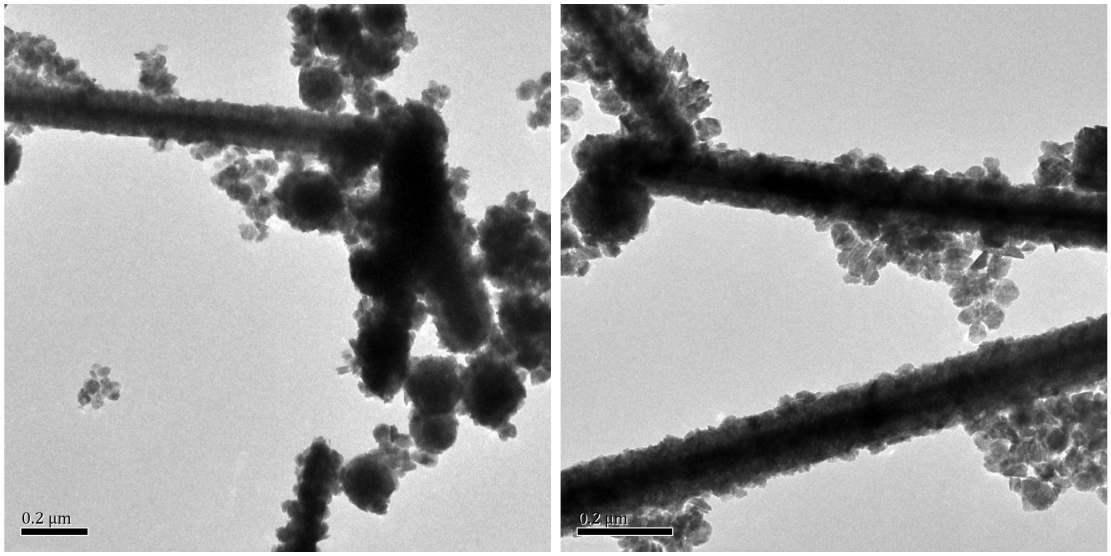

Fig. S15 TEM images of Cu-ZnO hybrid nanocrystals prepared using $CuCl_2$ instead of $Cu(acac)_2$ for the typical synthesis of Cu-ZnO core-shell nanoparticles.

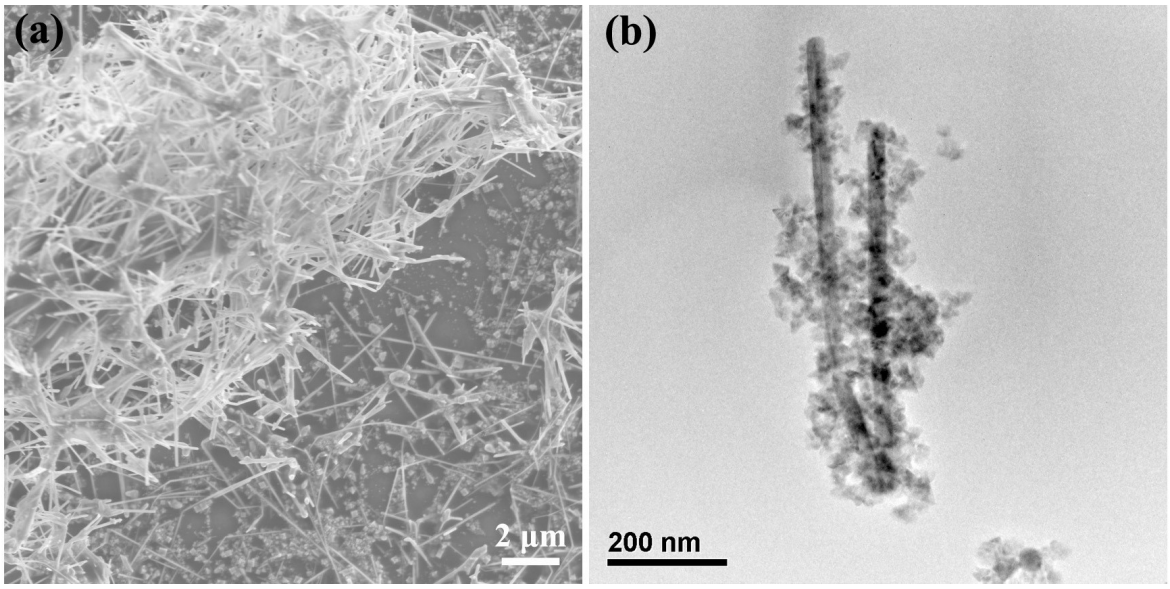

Fig. S16 SEM (a) and TEM (b) images of the products obtained using a two-step process in which the preformed uniform Cu nanowires prepared according to previous report[3] were washed at first and the remaining procedures are similar to those for the typical synthesis of Cu-ZnO core-shell nanowires.

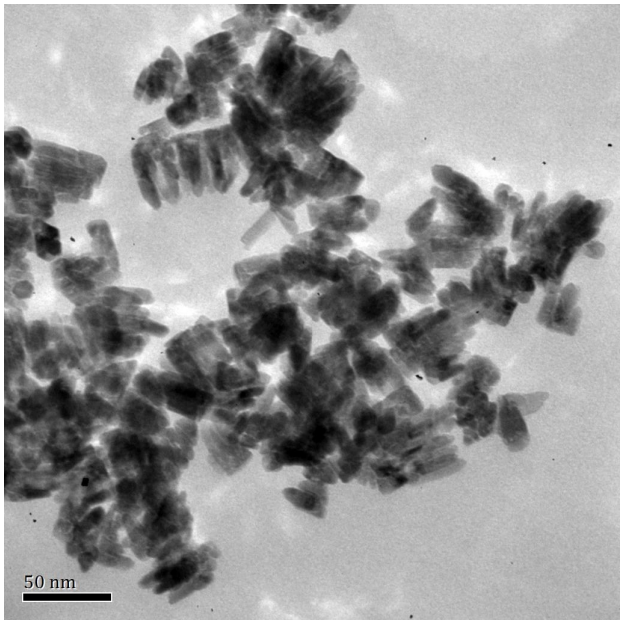

Fig. S17 TEM image of pure ZnO nanocrystals prepared using the similar method for preparing Cu-ZnO hybrid nanomultipods.

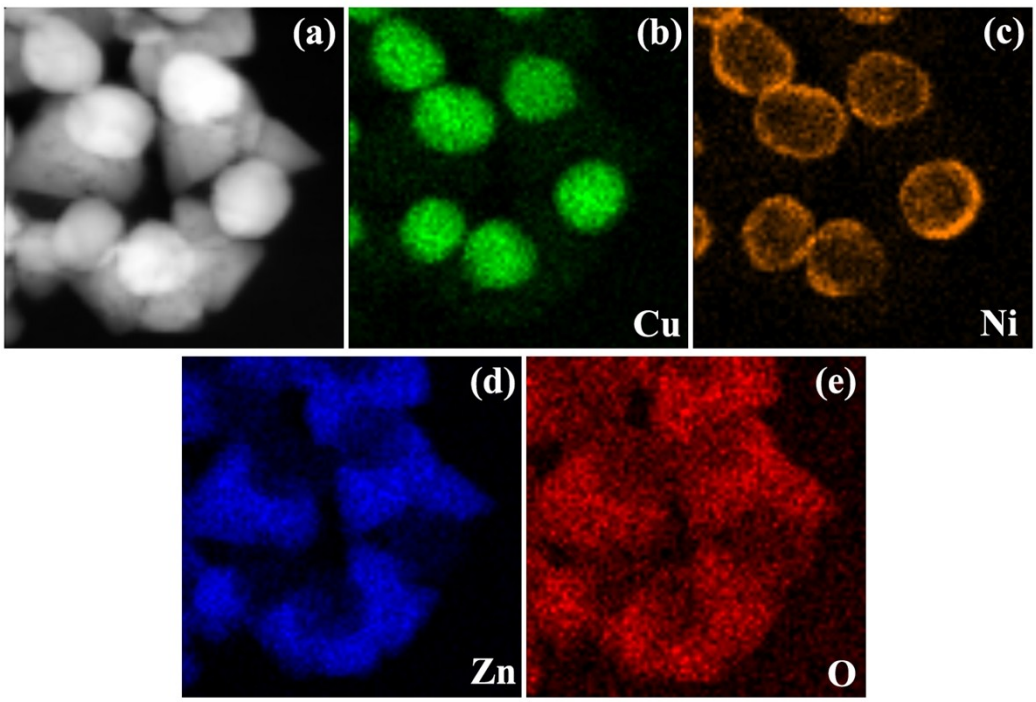

Fig. S18 HAADF image (a) along with elemental maps of Cu (b), Ni (c), Zn (d) and O (e) for Cu@CuNi-ZnO hybrid nanocrystals.

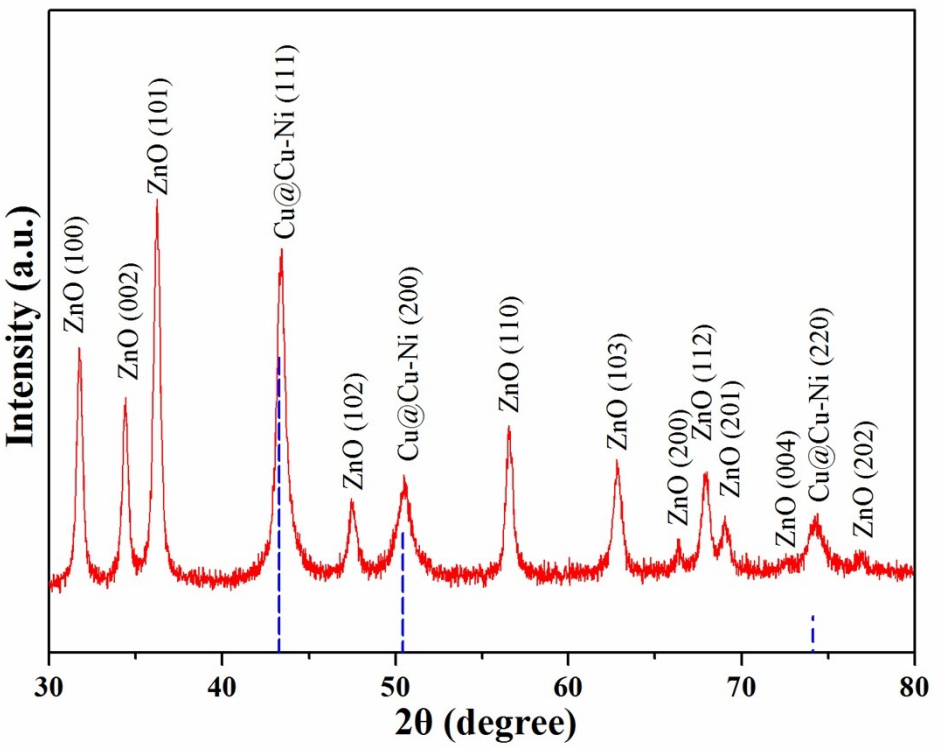

Fig. S19 XRD pattern of Cu@CuNi-ZnO hybrid nanocrystals. The standard pattern of fcc Cu (blue dotted line, JCPDS #04-0836) is included for comparison.

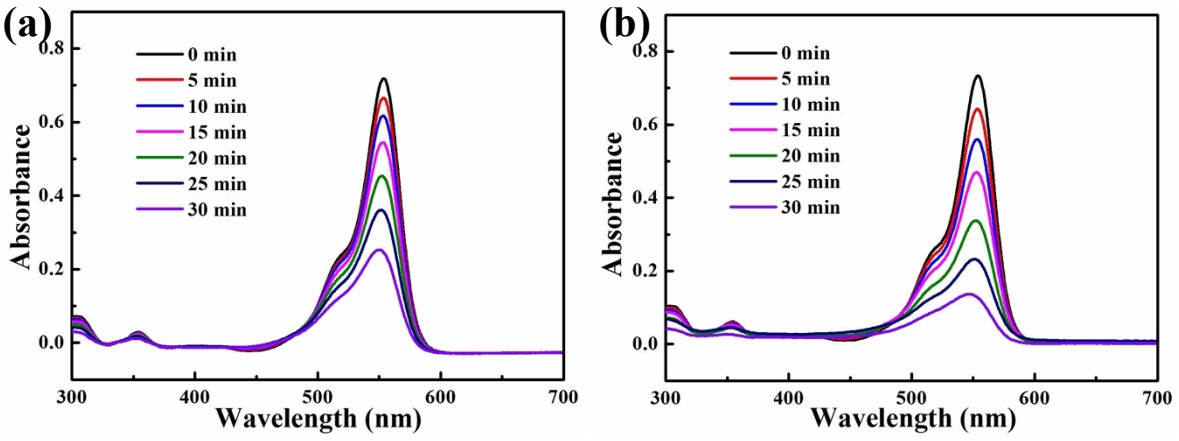

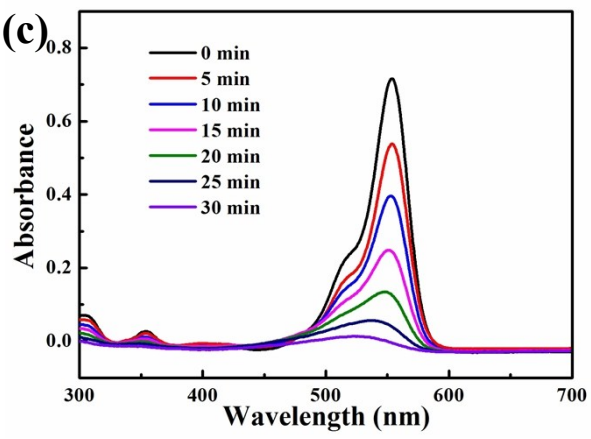

Fig. S20 Time-dependent UV-vis spectra recorded during the photocatalytic degradation of Rhodamine B by using pure ZnO nanocrystals (a), Cu@CuNi-ZnO hybrid nanocrystals (b), and Cu-ZnO hybrid nanomultipods (c).

References

1. I. S. Lee, N. Lee, J. Park, B. H. Kim, Y. W. Yi, T. Kim, T. K. Kim, I. H. Lee, S. R. Paik and T. Hyeon, *J. Am. Chem. Soc.*, 2006, **128**, 10658–10659.
2. M. N. Tahir, F. Natalio, M. A. Cambaz, M. Panthöfer, R. Branscheid, U. Kolbb and W. Tremel, *Nanoscale*, 2013, **5**, 9944–9949.
3. E. Ye, S.-Y. Zhang, S. Liu and M.-Y. Han, *Chem.–Eur. J.*, 2011, **17**, 3074–3077.

Table S1 Experimental parameters for the preparation of Cu-ZnO hybrid nanocrystals with different morphologies.

Sample morphology	**Cu precursor** (mmol)	**Solvent** (mL)	**Surfactant** (mmol)	**Temperature (1st/2nd Stage, °C)**	**ZnO precursor** (mmol)	**TEM image**
★Typical nanomultipods	$Cu(acac)_2$ (0.2)	OAm (3) BA (4)	TOPO (1.5)	195/195	$Zn(OAc)_2{\cdot}2H_2O$ (0.55)	Fig. 1
No hybrid nanocrystals	$Cu(acac)_2$ (0.2)	BA (4)	TOPO (1.5)	195/195	$Zn(OAc)_2{\cdot}2H_2O$ (0.55)	not shown
Cu-ZnO nanomultipods	$Cu(acac)_2$ (0.2)	OAm (5) BA (4)	TOPO (1.5)	195/195	$Zn(OAc)_2{\cdot}2H_2O$ (0.55)	Fig. S4a
Nanomultipods + nanorods	$Cu(acac)_2$ (0.2)	OAm (7) BA (4)	TOPO (1.5)	195/195	$Zn(OAc)_2{\cdot}2H_2O$ (0.55)	Fig. S4b
Liner Cu-ZnO nanorods	$Cu(acac)_2$ (0.2)	OAm (10) BA (4)	TOPO (1.5)	195/195	$Zn(OAc)_2{\cdot}2H_2O$ (0.55)	Fig. S4c
No hybrid Nanocrystals	$Cu(acac)_2$ (0.2)	OAm (10)	TOPO (1.5)	195/195	$Zn(OAc)_2{\cdot}2H_2O$ (0.55)	not shown
Flower-like nanomultipods	$Cu(acac)_2$ (0.2)	OAm (3) BA (4)	TOPO (1.5)	195/195	$Zn(OAc)_2{\cdot}2H_2O$ (0.75)	Fig. S5
Core-shell NPs	$Cu(acac)_2$ (0.2)	OAm (3) BA (4)	TOPO (1.5)	195/195	$Zn(St)_2$ (0.55)	Fig. S9
Cu-ZnO nanomultipods	$Cu(acac)_2$ (0.2)	OAm (3) BA (4)	None	195/195	$Zn(OAc)_2{\cdot}2H_2O$ (0.55)	Fig. S10
★Typical core-shell NPs	$Cu(acac)_2$ (0.2)	OAm (2) DBE (3)	DDL (1.5) TOPO (0.5)	205/265	$Zn(OAc)_2{\cdot}2H_2O$ (0.68)	Fig. 2
Cu-ZnO core-shell NPs	$Cu(acac)_2$ (0.2)	DBE (5)	DDL (1.5) TOPO (0.5)	205/265	$Zn(OAc)_2{\cdot}2H_2O$ (0.68)	Fig. S11
Nonuniform nanopyramids	$Cu(acac)_2$ (0.2)	OAm (2) DBE (3)	DDL (1.5) TOPO (0.5)	205/265	$Zn(St)_2$ (0.68)	Fig. S12
★Typical nanopyramids	$Cu(acac)_2$ (0.15)	OAm (7)	TOPO (0.5)	200/285	$Zn(St)_2$ (0.6)	Fig. 3
Cu-ZnO nanopyramids	$Cu(acac)_2$ (0.15)	OAm (7)	TOPO (1.5)	200/285	$Zn(St)_2$ (0.6)	not shown
No hybrid Nanocrystals	$Cu(acac)_2$ (0.15)	OAm (7)	TOPO (0.5)	200/285	$Zn(OAc)_2{\cdot}2H_2O$ (0.6)	not shown
★Typical core-shell NWs	$CuCl_2$ (0.02)	OAm (7)	TOPO (0.5)	200/290	$Zn(St)_2$ (0.5)	Fig. 4
Core-shell NRs+NPs	$CuCl_2$ (0.2)	OAm (3) BA (4)	TOPO (1.5)	195/195	$Zn(OAc)_2{\cdot}2H_2O$ (0.55)	Fig. S14
Core-shell NRs+NPs	$CuCl_2$ (0.2)	OAm (2) DBE (3)	DDL (1.5) TOPO (0.5)	205/265	$Zn(OAc)_2{\cdot}2H_2O$ (0.68)	Fig. S15